machines

MDPI

Article

Manufacturing Time Investigation for Double Wishbone Steering Knuckles in LCVs

Alexandru Dobre *, Vicentziu-Constantin Mihăilă, Gabriel Burduș and Răzvan-Alexandru Durigon

Automotive Engineering Department, National University of Science and Technology Politehnica Bucharest, 060042 Bucharest, Romania; vicentziu.mihaila@stud.trans.upb.ro (V.-C.M.); gabriel.burdus@stud.trans.upb.ro (G.B.); razvan.durigon@stud.trans.upb.ro (R.-A.D.)
* Correspondence: alexandru.dobre@upb.ro

Abstract

Light Commercial Vehicles (LCVs) need to be manufactured faster than ever, placing immense pressure on engineering teams to shorten development cycles. The double wishbone steering knuckle perfectly illustrates this challenge, as it must endure massive dynamic loads while keeping unsprung mass to an absolute minimum. In this paper, we explore a digital-to-physical workflow that drastically cuts down the time required to design and validate such critical suspension parts. We started by building a parametric baseline in CATIA, ensuring all kinematic hard points and packaging limits were strictly met, and to avoid the expense of immediate physical testing, we validated the design virtually using Finite Element Analysis (FEA). By subjecting the model to extreme LCV scenarios, including maximum braking torque, severe cornering, and harsh vertical impacts, we confirmed the structural safety factors. The article reflects that instead of waiting weeks for traditional CNC machining or sand casting, Additive Manufacturing (AM) can be used in the prototyping phase. Printing a polymer mock-up allowed us to instantly check for spatial interferences with the brake caliper and wheel hub. Finally, this approach proves that combining CAD, FEA, and 3D printing can reduce the automotive engineering cycle, turning digital concepts into physical mock-ups for packaging verification within hours.

Keywords: steering knuckle; finite element analysis; parametric optimization; additive manufacturing; rapid prototyping; functional mock-up

1. Introduction

1.1. Engineering Context and Development Challenges for LCV Steering Knuckles

The development of modern automotive chassis components is characterized by the need to satisfy several engineering requirements simultaneously, including structural integrity, kinematic performance, mass efficiency, manufacturability, cost, and development time. These requirements become particularly demanding in light commercial vehicles (LCVs), where the suspension system must accommodate substantial variations in payload while maintaining predictable vehicle behavior. Suspension is consequently required to perform under a wide range of operating conditions, from lightly loaded operation to the maximum authorized vehicle mass, while remaining capable of transmitting the forces generated during braking, cornering, road excitation, and other transient events. Within this system, the steering knuckle represents a critical structural and functional component because it provides the connection between the wheel-end assembly, steering mechanism,

Check for updates

Academic Editor: Kai Cheng

Received: 1 August 2026
Revised: 9 October 2026
Accepted: 14 October 2026
Published: 16 October 2026

Copyright: © 2026 by the authors. Licensee MDPI, Basel, Switzerland. This article is an open access article distributed under the terms and conditions of the Creative Commons Attribution (CC BY) license.

and suspension links and therefore participates directly in the transmission of forces and moments through the front axle [1–3].

The steering knuckle cannot be considered solely as a load-bearing structural member. Its geometry also defines important interfaces within the suspension assembly and consequently contributes to the kinematic behavior of the wheel. In a double-wishbone suspension, the upper and lower control arms constrain the motion of the upright, while the steering mechanism introduces an additional degree of control associated with wheel steering. The relative position of these attachment points determines the trajectory of the wheel during suspension travel and influences parameters such as camber, toe, caster, and steering behavior. Consequently, the design of a steering knuckle is inherently coupled with the geometry of the complete suspension system rather than being an isolated component-design problem [1,2].

The double-wishbone configuration is particularly suitable for applications in which control of suspension kinematics is important because the use of two independently articulated control arms allows the wheel motion to be defined through a relatively large number of geometric parameters. This flexibility, however, also increases the number of constraints that must be satisfied during component development. A change in the position of one attachment point may alter the motion of the wheel throughout the suspension stroke and may consequently affect several kinematic quantities simultaneously. Computational representations of double-wishbone systems have therefore become useful for studying suspension motion and for evaluating the relationship between geometric parameters and vehicle-level behavior [4,5]. Recent computational work further demonstrates the value of parameterized three-dimensional models for representing double-wishbone mechanisms and investigating their kinematic response under different configurations [4].

For an LCV, the geometric problem is further complicated by the variation in operating conditions associated with vehicle payload. The vertical loads transmitted through the suspension change with vehicle mass, while braking and cornering loads introduce longitudinal and lateral force components. The resulting load combinations can produce significant bending and torsional effects within the steering knuckle. Vehicle-dynamics analysis consequently provides an essential basis for defining the loading environment in which a suspension component must operate. Rather than relying on a single nominal load, the design process should consider representative combinations of vehicle operating conditions so that the structural assessment remains connected to the actual function of the component [3,5].

The structural requirements imposed by these loading conditions must be reconciled with the mass of the component. The steering knuckle forms part of the unsprung assembly, meaning that unnecessary material contributes to unsprung mass without directly improving the intended structural function. Reducing this mass can therefore be an important objective in suspension component development. At the same time, weight reduction cannot be pursued independently of strength and stiffness because excessive material removal may increase deformation, generate local stress concentrations, or compromise the durability and safety of the component. The engineering problem is thus one of constrained lightweight design: material should be removed only where the resulting geometry continues to satisfy the required structural and functional conditions [6–8].

This balance between structural performance and mass has led to extensive use of finite element analysis (FEA) in the development of automotive suspension components. FEA enables stress and deformations to be evaluated for complex three-dimensional geometries under loading conditions that would otherwise require physical prototypes for experimental assessment. For steering knuckles and related suspension components, FEA has been repeatedly employed to identify critical stress regions and to assess the possibility

of reducing material while maintaining an acceptable safety margin [6–8]. The usefulness of such analyses depends strongly on the quality of the model definition, including the representation of the suspension interfaces, material properties, mesh, constraints, and applied loads. A numerical result is therefore meaningful only when the simulated configuration adequately represents the intended physical operating condition.

The development of steering knuckles has also increasingly incorporated structural optimization techniques. Topology optimization provides a systematic method for determining an efficient distribution of material within a predefined design domain subject to structural constraints. In automotive applications, this approach can reveal regions in which material contributes comparatively little to the structural response and can consequently provide a basis for developing lighter geometries. Recent investigations specifically addressing steering-knuckle design have demonstrated the potential of topology optimization to achieve substantial reductions in mass while maintaining the required structural response [6,7]. Such results are particularly relevant to suspension components because they illustrate how computational structural analysis can be transformed from a verification tool into an active part of the geometry-development process.

Optimization algorithms do not eliminate the need for engineering interpretation. The geometry generated by an optimization procedure must be reconciled with the kinematic interfaces, assembly requirements, manufacturing limitations, and geometric constraints of the actual component. This is especially important for a steering knuckle because the optimized region cannot interfere with the wheel hub, brake system, control arms, steering linkage, or surrounding chassis components. Consequently, a practical optimization workflow must preserve the functional geometry of the component while allowing structural material to be redistributed in regions where such modification is feasible. Recent steering-knuckle research combining topology optimization with subsequent manufacturing processes illustrates the increasing importance of considering structural optimization and manufacturability as interconnected design decisions rather than independent stages [7].

The physical realization of an optimized geometry represents another important stage in the development process. Conventional prototype manufacturing can involve casting patterns, molds, dedicated fixtures, machining operations, and other preparatory activities. These requirements can become particularly restrictive when several design iterations are necessary. Additive manufacturing (AM) provides an alternative route for producing physical prototypes directly from digital geometry and is therefore particularly attractive during early-stage development. The principal advantage in this context is not necessarily the immediate production of a final load-bearing component, but the ability to convert a revised digital model into a physical representation without the tooling requirements associated with many conventional manufacturing processes [9,10].

Design for additive manufacturing has consequently developed into a broader engineering discipline concerned with the relationship between component geometry, manufacturing process, material behavior, and production requirements. The design freedom associated with AM can support complex geometries and rapid design iteration, while the direct conversion of digital models into physical parts can reduce the time required for prototype preparation and manufacturing. However, the process also introduces specific constraints related to build orientation, support structures, dimensional accuracy, surface quality, material properties, and production efficiency [9]. For this reason, the use of AM in automotive development should be considered in relation to the specific purpose of the prototype. A polymer prototype, for example, may not possess the mechanical properties required for direct structural operation but can nevertheless provide valuable information concerning geometric fit, accessibility, component interference, and assembly feasibility.

The possibility of using AM as part of a digital-to-physical development cycle has become increasingly relevant to automotive engineering. Recent research on automotive prototypes identifies the integration of computer-aided design and additive manufacturing as a means of shortening the transition between digital design and physical verification while also enabling more flexible iteration of complex geometries [10]. More recent work on optimized steering knuckles has extended this concept by combining computational optimization with additive manufacturing and subsequent manufacturing processes, illustrating the growing tendency to treat digital design, optimization, and fabrication as interconnected activities [7].

Literature therefore establishes several important aspects of the problem addressed in the present study. Suspension research provides established methods for understanding double-wishbone kinematics and the influence of geometric parameters on wheel motion [1,4,5]. Structural-analysis research demonstrates the applicability of FEA to suspension-component assessment and lightweight design [6–8]. In parallel, AM research has established the potential of digitally driven manufacturing for accelerating prototype development and enabling complex geometries to be produced without conventional tooling [9,10]. These research directions are complementary, but their practical integration remains an important engineering consideration, particularly when the objective is not merely to optimize a component numerically but to establish a continuous workflow from kinematic definition through structural verification and physical packaging validation.

This issue is particularly relevant to the development of an LCV steering knuckle, where the geometric constraints of a double-wishbone suspension, the severe loading conditions associated with commercial-vehicle operation, the requirement for controlled unsprung mass, and the need for rapid physical verification must all be addressed simultaneously. A development strategy that considers these requirements separately can lead to repeated transfers between CAD modelling, numerical analysis, redesign, and prototype manufacturing. Conversely, integrating these stages can establish a more direct relationship between the digital model, its structural response, and its physical implementation. The present study is therefore positioned within this integrated design context, using a parametric CAD representation to establish the suspension geometry, FEA to assess structural behavior and guide material reduction, and additive manufacturing to produce a physical mock-up for rapid geometric and packaging validation.

The resulting research problem is not simply whether a steering knuckle can be made lighter or whether additive manufacturing can produce a prototype. Both questions have already been addressed independently in the literature [6–10]. The more specific issue is whether these technologies can be organized into a coherent development sequence for an LCV double-wishbone steering knuckle in which kinematic requirements are established first, structural performance is subsequently verified and used to guide geometric refinement, and the resulting geometry is then transferred rapidly into a physical prototype for packaging assessment. This integrated perspective defines the context for the subsequent review of suspension kinematics, structural analysis, optimization strategies, and additive manufacturing technologies.

1.2. Double-Wishbone Suspension Architecture and Steering-Knuckle Kinematics

The double-wishbone suspension remains an important architecture for applications in which control of wheel kinematics and suspension geometry is required. Its configuration, based on upper and lower control arms connecting the wheel carrier to the vehicle structure, provides a comparatively large number of geometric design variables and consequently allows the wheel trajectory and alignment characteristics to be tailored to the intended vehicle application [11,12]. Recent computational studies continue to employ three-dimensional

parametric models of the double-wishbone mechanism because its spatial geometry directly determines the position and orientation of the wheel carrier throughout suspension travel [11,13].

The principal geometric variables are the suspension hardpoints, including the inner control-arm pivots, ball-joint locations, wheel center, and steering-link connections. Their coordinates determine the motion of the steering knuckle and influence parameters such as camber, toe, caster, and kingpin inclination. Recent optimization studies have demonstrated that modifying these coordinates can improve several kinematic characteristics simultaneously, although the objectives remain coupled and therefore require multi-objective treatment [14–16]. Zhang et al., for example, developed a multi-objective optimization procedure for the hardpoint parameters of a double-wishbone independent suspension, while Sun et al. used ADAMS-based optimization to improve the variation in toe, camber, caster, and kingpin inclination during wheel travel [14,15].

The spatial and nonlinear character of the mechanism also makes an accurate three-dimensional representation important. Niu et al. addressed this problem by developing an explicit solution for the nonlinear geometry of a double-wishbone suspension, separating the steering and wheel-jumping degrees of freedom to improve the computational treatment of the mechanism [17]. The importance of considering the actual elastokinematic behavior of the suspension has also been demonstrated in recent multibody modelling research, in which double-wishbone systems were represented together with flexible connections and nonlinear bushing characteristics [18]. Such approaches are relevant because the actual wheel position can depend not only on idealized rigid-body geometry but also on the compliance of the suspension components and joints.

Recent work has further extended suspension optimization toward integrated and computationally efficient design. Llopis-Albert et al. combined CAD, FEA, and multibody simulation within a multi-objective optimization framework for a front double-wishbone suspension, demonstrating the value of linking geometric, structural, and dynamic analyses within the same design process [19]. Nishikawa et al. similarly addressed the large number of constraints and design variables associated with double-wishbone suspension design through a set-based approach using differential evolution and adaptive sampling [20]. More recent research has also applied multi-fidelity and data-driven optimization to suspension-mechanism design, including different double-wishbone configurations [21], while a 2026 study specifically optimized double-wishbone hardpoints and wheel-alignment parameters using multibody dynamics and sensitivity analysis [22].

For the steering knuckle, these findings establish the hardpoint geometry as a fundamental functional constraint. The interfaces with the upper and lower control arms, wheel hub, and steering system determine the position and motion of the component and must therefore be preserved when its structure is subsequently optimized. The kinematic model consequently provides the geometric framework within which the structural design of the knuckle can be performed. This distinction is particularly important for lightweighting: material can be redistributed within the available design space, but modifications that alter the functional hardpoints may change the suspension kinematics and therefore the intended vehicle behavior [14–17].

For the present study, the double-wishbone configuration is consequently considered first from a kinematic perspective, with the steering-knuckle interfaces defining the functional geometry of the component. Once this geometry is established, the structural performance of the knuckle can be assessed under representative loading conditions. Establishing these constraints at the digital stage reduces the need for premature physical iterations and provides a more efficient basis for the subsequent structural development process. This provides the basis for the next stage of the development process, in which

finite element analysis is used to identify critical regions and investigate opportunities for structural optimization.

1.3. Structural Assessment and Weight Reduction Using FEA

Finite Element Analysis (FEA) has become a fundamental tool for assessing automotive suspension components because it enables structural response to be evaluated before physical prototypes are manufactured. For steering knuckles, this capability is particularly important because the component transfers forces between the wheel hub, suspension links, steering system, and braking assembly. Its design must satisfy strength and stiffness requirements while avoiding unnecessary material and unsprung mass. Recent studies confirm the usefulness of FEA for both preliminary strength assessment and lightweight design of automotive knuckles [21–24].

A reliable FEA study begins with an appropriate representation of the physical system. The CAD geometry must capture principal load paths and critical interfaces, while insignificant features may be simplified for meshing. Boundary conditions should reproduce the actual constraints at the suspension and wheel interfaces, and applied loads should represent realistic service events. Studies combining vehicle dynamics with finite element models show that knuckle loads vary with road excitation, braking, cornering, and steering maneuvers [22,23]. This is relevant to LCVs, where payload variation can generate severe multi-axial loading.

The principal outputs of static structural analysis are equivalent von Mises stress, total deformation, and factor of safety. For ductile metals, comparing maximum equivalent stress with yield strength provides a first indication of resistance to permanent deformation. Static strength, however, is not sufficient for a safety-critical suspension component. Repeated service loading can produce fatigue damage even when stress remains below yield. Recent research therefore combines FEA with fatigue assessment, emphasizing variable-amplitude and multi-axial loading histories [22,23]. Material substitution also requires consideration of stiffness and fatigue behavior; aluminum knuckle designs require structural and durability verification in addition to mass reduction [21].

After baseline validation, FEA can identify low-utilization regions and guide material removal. This provides the basis for topology and shape optimization, where material is redistributed toward efficient load paths while structural constraints are maintained. Recent steering-knuckle investigations have demonstrated mass reductions through topology optimization while preserving acceptable stress and safety-factor levels [24,25]. Optimization must nevertheless preserve functional interfaces, wall thickness, manufacturability, and adequate stiffness. The mechanically optimal geometry is therefore not necessarily the most practical for production.

This consideration becomes important when lightweighting is followed by additive manufacturing. Process-aware topology optimization can incorporate manufacturing constraints, so the geometry remains compatible with the intended production route [25,26]. Recent work has demonstrated the potential of combining topology optimization with AM-oriented design for steering knuckles, enabling complex load-bearing geometries with reduced material usage [24]. Multi-objective approaches can also consider structural performance, material selection, and manufacturing requirements simultaneously [27].

Accordingly, FEA should be treated not only as a final verification method but also as an iterative design instrument linking load definition, structural validation, and weight reduction. In the present LCV study, a conservative baseline is first assessed under severe load cases, after which low-stress regions are progressively removed and each geometry is re-evaluated. Such an iterative strategy provides a controlled basis for reducing unsprung mass while retaining structural safety and required kinematic functionality [28–30].

1.4. From Conventional Prototyping to Additive Manufacturing

The physical validation of automotive components has traditionally depended on manufacturing routes such as casting and CNC machining. These methods remain indispensable when prototypes must reproduce the material properties and mechanical performance of the final component. However, conventional prototype production may require patterns, molds, dedicated fixtures, machining programs, and multiple processing stages. Consequently, when the geometry is modified during development, each iteration can generate additional preparation time and cost. For geometrically complex components such as steering knuckles, this can slow the transition from numerical design to physical verification.

Additive manufacturing (AM) provides an alternative by enabling physical components to be fabricated directly from digital geometry without dedicated part-specific tooling. Recent literature shows that AM is increasingly used in the automotive sector for prototyping, tooling, lightweight structures, customized parts, and selected end-use applications [31–35]. Its importance during product development is primarily associated with design flexibility and the possibility of rapidly converting revised CAD models into physical objects. This capability is particularly valuable when several design iterations are required before structural, packaging, assembly, and manufacturing requirements are simultaneously satisfied.

The transition from conventional to additive prototyping also changes the relationship between geometry, manufacturability and final production time. Conventional processes impose constraints associated with tool accessibility, parting surfaces, draft angles, and machining paths. AM can accommodate more complex geometries and, in some cases, enable material to be placed closer to the required load paths. Nevertheless, additive processes introduce their own constraints, including build orientation, supporting generation, dimensional accuracy, surface quality, thermal effects, post-processing, production cost, production time and process reliability. Design for Additive Manufacturing has therefore become an important consideration when transferring optimized digital geometries into physical components [36–38].

For automotive structural components, the intended function of the prototype is particularly important. Metal AM can support the fabrication of complex load-bearing parts, but its application may involve higher equipment costs, specialized materials, process control, and post-processing requirements [33,39]. Polymer-based AM offers a more accessible route when the primary objective is rapid geometric and assembly validation rather than direct structural service. Such prototypes can be used to assess spatial clearances, component interference, accessibility, assembly sequence, and the preservation of functional interfaces before committing to more expensive manufacturing routes.

This distinction is directly relevant to steering-knuckle development. A polymer prototype cannot reproduce the fatigue resistance or load-carrying capability of the final metallic component and should therefore not replace structural verification. Instead, AM can complement CAD and FEA by introducing a rapid physical-validation stage. The same geometry that has been developed and structurally assessed in the digital environment can be fabricated and examined within the actual suspension assembly, allowing packaging problems that are not readily apparent from numerical results alone to be identified.

Literature therefore indicates a transition from a sequential development process toward a more integrated digital-to-physical workflow. Conventional manufacturing remains necessary for functional and production-intent components, whereas AM is particularly advantageous when rapid iteration and early physical validation are required [31–40]. For the present study, AM is consequently considered as a rapid-prototyping tool positioned after the definition of the steering-knuckle geometry and its structural assessment. This

approach supports the subsequent integration of CAD, FEA, and physical prototyping into an efficient and continuous development workflow, aimed at reducing development and prototyping time while forming the basis for identifying the remaining research gap.

1.5. Integration of CAD, FEA and AM: Current State and Research Gap

The increasing digitalization of engineering design has encouraged a closer integration of computer-aided design (CAD), finite element analysis (FEA), and additive manufacturing (AM). Rather than operating completely independent activities, these tools can form a continuous workflow in which geometry creation, structural assessment, design modification, and physical realization are linked through iterative feedback. Recent studies on Design for Additive Manufacturing (DfAM) emphasize that the greatest potential of AM is achieved when manufacturing requirements are considered during the design process rather than after a geometry has already been finalized [41–43]. In this context, CAD provides the parametric description of the component, FEA evaluates its expected structural response, and AM enables the resulting geometry to be transferred rapidly into physical form.

However, the integration of these stages remains incomplete in many engineering applications. Conventional workflows often follow a sequential pattern in which a component is designed in CAD, subsequently analyzed, and only afterwards modified to satisfy manufacturing constraints. Such an approach can create repeated exchanges between design and analysis environments and may require substantial manual intervention when geometry changes invalidate previous meshes, boundary conditions, or manufacturing preparations. Recent research has therefore focused on automation and continuous data exchange between CAD, CAE, topology optimization, and AM-oriented design tools [44–47]. These approaches seek to reduce the discontinuities between design stages and to make structural and manufacturing constraints visible earlier in the development process.

Further development concerns the incorporation of AM-specific constraints directly into optimization and analysis procedures. Structural optimization alone may generate geometries that are theoretically efficient but difficult to print, requiring extensive support, post-processing, or redesign. DfAM-aware methodologies consequently attempt to consider functional performance and manufacturing limitations simultaneously. Nevertheless, recent reviews indicate that the available methods remain fragmented, with many approaches concentrating on individual phases of the design process rather than establishing a fully connected workflow from initial geometry definition to manufacturing and validation [41,42].

For automotive component development, this limitation is particularly relevant. The design of a steering knuckle requires simultaneous consideration of suspension interfaces, steering geometry, load transfer, structural performance, manufacturability, and physical packaging. Existing studies frequently address these aspects separately: suspension studies concentrate on kinematics, structural investigations focus on stress or fatigue behavior, while AM research often addresses prototype fabrication or process-specific design. Although these individual contributions provide valuable knowledge, fewer studies demonstrate an accessible end-to-end workflow that explicitly connects parametric CAD modelling, FEA-based structural verification, iterative geometry refinement, and rapid physical validation for a suspension component.

The research gap addressed in the present study therefore concerns the practical integration of these established tools within a single and reproducible development sequence. Rather than proposing a new optimization algorithm or replacing conventional manufacturing with AM, the study investigates how CAD, FEA, and polymer-based additive prototyping can be combined to support the development and validation of a lightweight

steering knuckle. The resulting workflow links digital geometry, structural evaluation, and physical assembly verification, providing a basis for the methodological contribution defined in the following section [47–50].

1.6. Aim and Contribution of the Present Study

The aim of the present study is to investigate an integrated engineering workflow for reducing the development and prototyping time of a steering knuckle intended for a light commercial vehicle equipped with a double-wishbone suspension. The proposed approach combines parametric CAD modelling, finite element analysis (FEA), iterative geometry refinement, and additive manufacturing-based physical prototyping within a unified development sequence. By connecting these activities rather than treating them as independent stages, the methodology is intended to streamline the transition from functional suspension geometry to structural assessment and physical prototype validation. The main contribution of this work is therefore methodological with particular emphasis on the integration of digital design, structural evaluation, and rapid physical prototyping. First, the steering-knuckle geometry is defined according to the functional requirements and interface constraints imposed by the suspension and steering architecture. Second, the structural response is evaluated using FEA under representative loading conditions, allowing critical regions and opportunities for weight reduction to be identified. The geometry is subsequently refined through an iterative design process while preserving the required mechanical interfaces and functional characteristics. Finally, the resulting CAD model is transferred to an additive-manufacturing process to produce a physical prototype for the verification of geometric compatibility, packaging, accessibility, and assembly conditions.

By integrating these activities into a continuous development sequence, the proposed workflow addresses the time associated with repeated transitions between design, structural verification, and physical prototyping. Rather than focusing exclusively on suspension kinematics, structural optimization, or additive manufacturing, the present work integrates these complementary approaches within a single workflow applied specifically to steering-knuckle development. The study therefore demonstrates how digital design and structural simulation can relate to rapid physical validation, supporting faster design iteration and reducing the risk of discovering assembly-related problems only at later stages of development.

2. Materials and Methods

2.1. Suspension Architecture Requirements

The geometric and kinematic baseline for the analyzed steering knuckle was derived from an existing LCV from the N1 category, Iveco Daily III manufactured by Fiat S.p.A., Turin, Italy. The vehicle is equipped with an independent front suspension with transversal double wishbone mechanism and horizontal unequal control arms. The boundary conditions depend on the mass parameters, so we established the conditions to be for the Maximum Authorized Mass of 3.5 t. All the kinematic hard points, as well as the load cases (maximum braking torque, cornering lateral forces and dynamic obstacle impacts), were chosen to support the final total weight.

2.2. Kinematic Parametrization and Load-Case Determination

We analytically determined the basic geometric and dynamic parameters of the steering knuckle based on the 3.5-t vehicle architecture. These parameters were used to make the digital model in CATIA V5 R20 and to set the boundary conditions for the Finite Element Analysis (FEA).

The kinematic hardpoints of the double wishbone mechanism dictate the overall height of the upright, and according to the analytical baseline, the vertical distance between the upper and lower control-arm ball joints was established at h = 230 mm, with the wheel center positioned at b = 100 mm above the lower articulation. To accommodate the heavy-duty wheel hub bearing assembly, the critical spindle diameter was sized to D_s = 50 mm, ensuring a sufficient safety margin against bending fatigue, while the interior diameter of the knuckle is D_{ki} = 80 mm.

The FEA load cases were derived from real-world operational regimes rather than executing purely theoretical structural optimization, and the analytical model evaluated three primary scenarios: severe braking, cornering lateral forces and dynamic obstacle impact. The mathematical evaluation revealed that the obstacle impact regime generates the highest stress concentrations. We applied a dynamic amplification factor (k_d = 2) to all forces taken into consideration. These maximum forces, along with the maximum bending moment calculated at the critical spindle section, are the primary boundary conditions introduced into the SimScale static linear analysis. The values of these forces are shown in Table 1. This way, the optimized component will withstand the most severe payload fluctuations relevant for N1-category vehicles.

Table 1. Boundary conditions used in the simulation.

Loading Conditions	Symbol	Values
Vertical reaction at the right tire contact patch	Z_r	14,537 N
Longitudinal force at the right contact patch	X_r	5451 N
Maximum bending moment	M_b	327 N·m

The vertical reaction at the right tire contact patch has the following formula:

$$Z_r = k_d \cdot \frac{Z_1}{2} \tag{1}$$

where Z_1 is the equivalent load on the front axle. The force is calculated knowing the coordinates of the vehicle's center of gravity, which is determined considering the center of gravity of each individual component shown in Figure 1. The passengers and the cargo were also taken into consideration, with the resulting center of gravity being closer to the rear axle.

The vertical reaction at the right contact patch is shown in Figure 2.

The total load on both axles is equivalent to 3.5 t or 34,335 N. The center of gravity is positioned between the two axles, 1503 mm from the rear axle and 2047 mm from the front axle. In this case, the front axle load will be calculated using the formula:

$$Z_1 = \frac{b}{a+b} \cdot G \tag{2}$$

In practice, the dynamic amplification factor can be anywhere between 1.5 and 3. It depends on the type of suspension system, the type of vehicle and the type of obstacle or pothole. For example, in motorsport, it can reach up to 5, which leads to a dynamic load that is 5 times the static load as shown by the authors of [51]. Bearing in mind the theme of this article refers to LCV's, a coefficient of 2 was considered.

The obstacle impact regime load case was considered critical due to the high transient vertical wheel loads associated with road irregularities. Experimental and numerical studies

have shown that severe road excitations can produce significantly higher vertical wheel loads than those associated with lateral or longitudinal vehicle maneuvers [52].

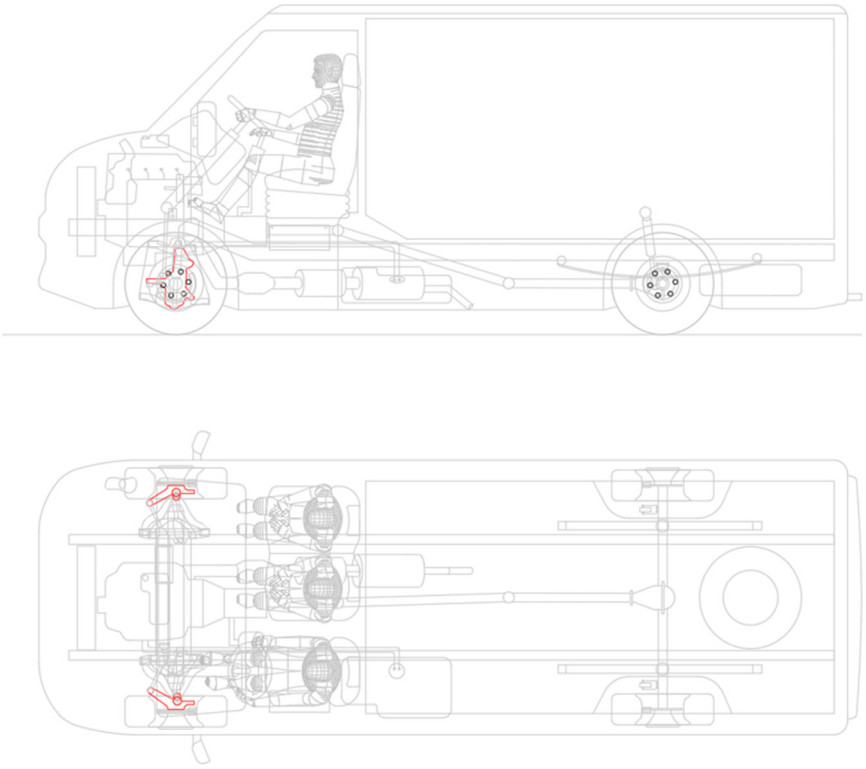


Figure 1. General organization of an LCV with the steering knuckles highlighted. The **top part** of the figure shows the longitudinal side view of the van, while the **bottom part** shows the top view.

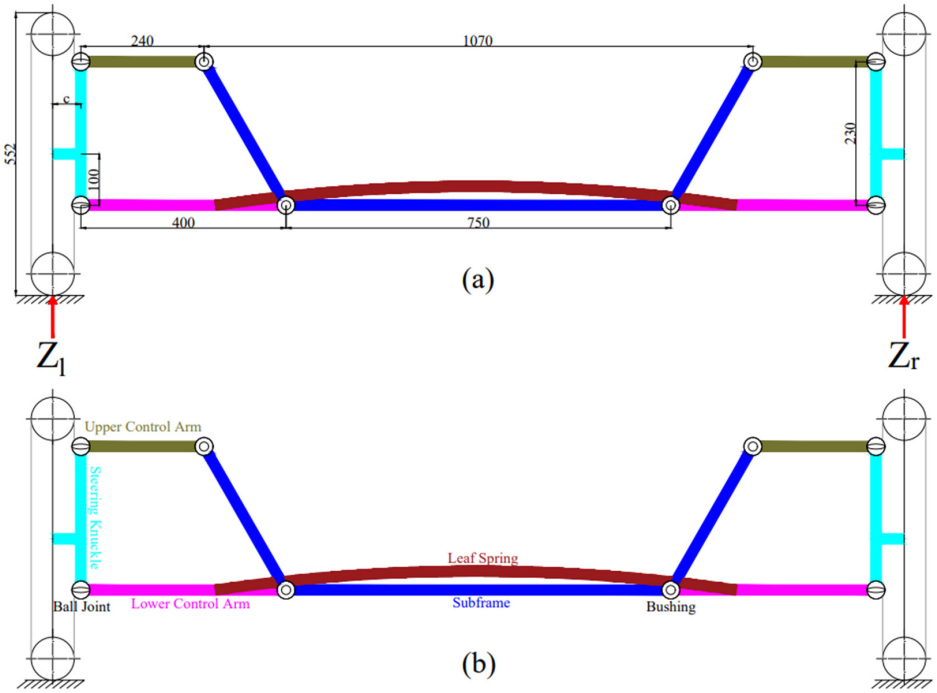


Figure 2. Principal dimensions and forces used for the kinematic and load-case definition (**a**) and simplified geometric representation of the main components of the double-wishbone front axle (**b**). Z_l and Z_r denote the vertical reactions at the left and right tire contact patches, respectively.

The longitudinal force at the right contact patch was calculated using the following formula:

$$X_r = \varphi_x \cdot \frac{Z_1}{2} \quad (3)$$

where φ_x is the longitudinal tire friction coefficient. The coefficient depends on the condition of the tire and the road. It can only have values lower than 1. A coefficient of 0.75 was used in the calculus.

The maximum bending moment corresponds to the vertical reaction load and has the following formula:

$$M_b = Z_r \cdot c \quad (4)$$

where c is the distance between the vertical symmetry plane of the wheel and the critical section of the steering knuckle.

2.3. Digital Modelling

The digital making of the steering knuckle was executed within the CATIA V5 Part Design environment using a parametric approach. The primary solid volume was constructed via basic additive operations like Pad and Shaft, explicitly dimensioned to accommodate a separate, standardized hub and double bearing assembly and to eliminate bulk material and refine the initial geometry, we used subtractive features like Pocket. To reduce stress concentrators, which are critical for high-load suspension components, all structural transitions were smoothed utilizing edge fillets and chamfers. This modelling strategy ensures a continuous flow of the 3D model and prepares the solid body for accurate finite element discretization, which was done directly in SimScale.

After the 3D modelling phase, we generated a 2D technical drawing to document the critical kinematic hard points, as shown in Figure 3. A section view of the knuckle is provided in Figure 4. This drafting phase geometrically validates the spatial packaging constraints and details the exact connection nodes for the control arms and the steering tie rod. The resulting unoptimized CAD model is a strict structural baseline for the project and instead of employing automated topological algorithms, this baseline will undergo an iterative parametric optimization, where material will be manually and strategically removed from low-stress regions identified during the stress analysis undergone in SimScale.

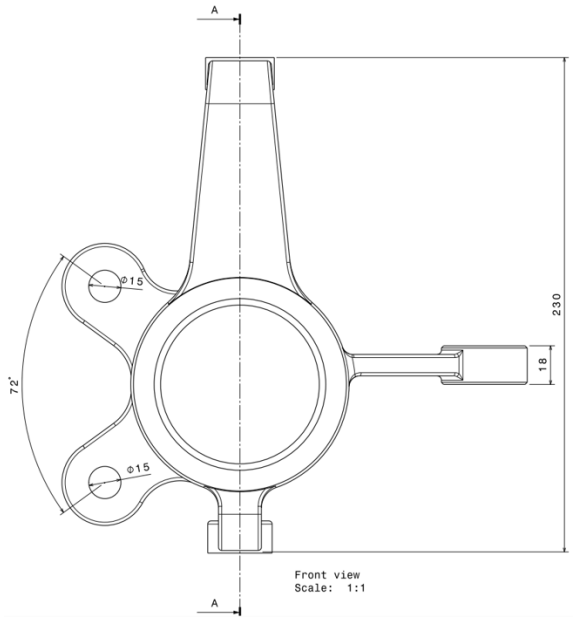


Figure 3. Front view of the 3D modelled steering knuckle.

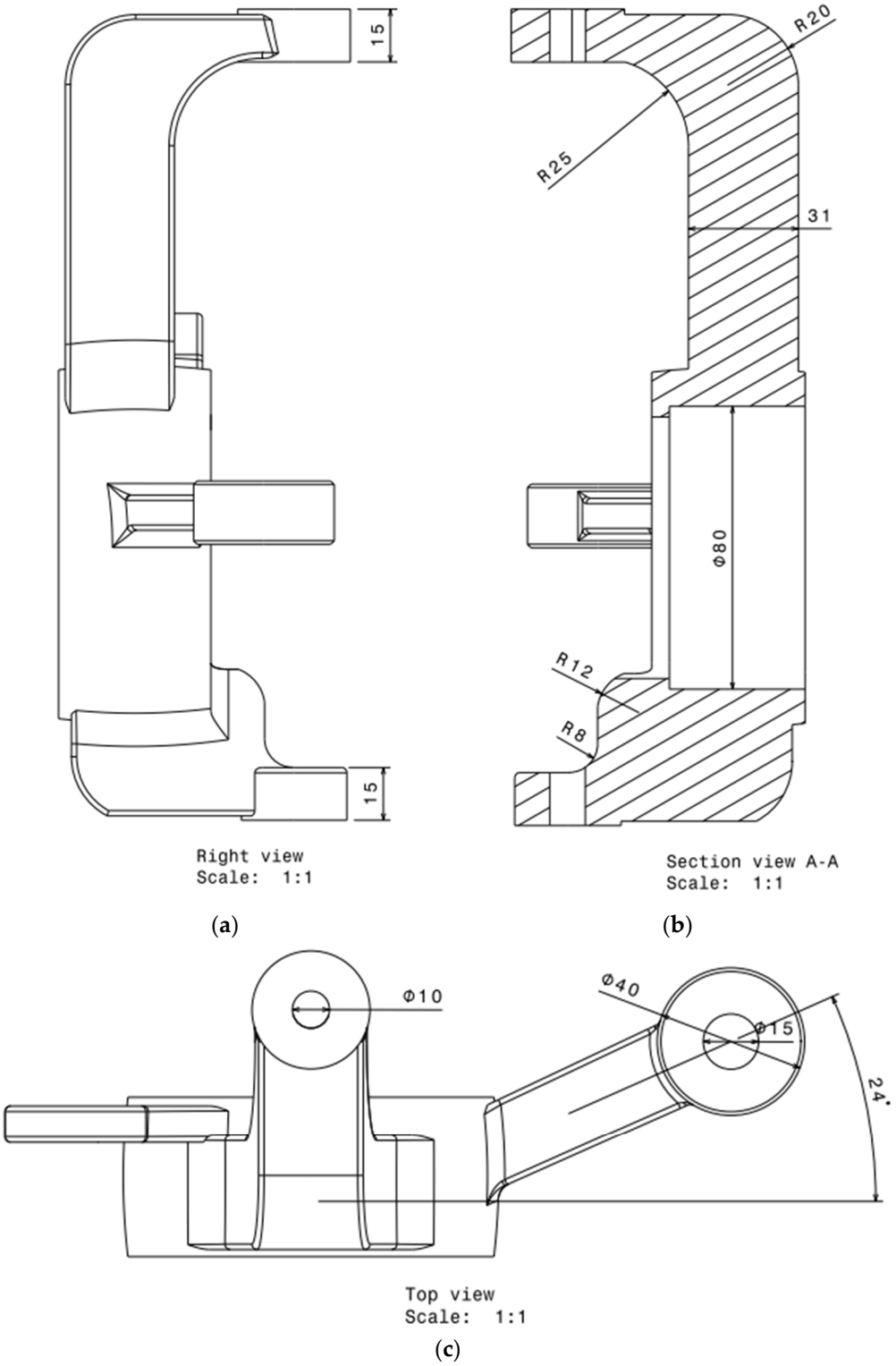


Figure 4. (**a**) Right view, (**b**) section view and (**c**) top view of the 3D-modelled steering knuckle.

2.4. Finite Element Analysis

The static linear structural analysis was performed using the SimScale cloud environment, on the official website using a free subscription account. The first crucial step was defining the material properties, so we assigned the mechanical characteristics of EN-GJS-450-10 nodular cast iron to the steering knuckle. This material is the industry standard for such suspension components due to optimal balance between a high yield strength, good

ability to casting, and superior vibration damping capabilities. The properties of the chosen material can be seen in Table 2.

Table 2. EN-GJS-450-10 nodular cast iron properties.

EN-GJS-450-10	Values
Density	7100 kg/m^3
Poisson's ratio	0.27
Young's modulus	1.69·10^5 MPa
Yield strength	310 MPa

To generate the finite element mesh, we used the imbedded mesh generator from SimScale. The mesh was produced utilizing second-order tetrahedral elements. This selection is imperative in structural simulations to prevent shear locking phenomena and to capture local stress gradients without inducing artificial stiffening in the model. In addition to the normal parameters of the mesh generator, we included a gap refinement factor of 0.05 to reduce the number of concentrators. The global mesh gradation rate was explicitly set to 1.22 to strictly control the spatial transition of the mesh density. According to established finite element meshing guidelines [53], the edge-length transition ratio between adjacent elements should be strictly constrained within the 1.20 to 1.25 range. Exceeding these theoretical limits can lead to ill-conditioned stiffness matrices and numerical interpolation errors across element boundaries. By selecting a gradation factor of 1.22 (restricting maximum growth to 22%), the discretization sits precisely within this optimal recommended window. This specific value guarantees a smooth, mathematically stable transition of the stress contours from the highly refined transition fillets to the larger elements of the bulk body while still allowing the mesh to coarsen sufficiently in low-stress regions to preserve computational efficiency. Furthermore, to accurately resolve the stress gradient at the critical fillet transition of the lower control arm mounting bracket, a minimum of three element layers were explicitly allocated across the thickness of the geometric feature.

To guarantee that the computed stress results are mesh-density independent, a rigorous mesh convergence study was conducted on the baseline model. Following standard FEA practices, the global mesh density was incrementally scaled across four discrete integer levels utilizing the solver's native fineness algorithm. A relative change of less than 5% in the peak von Mises stress between successive mesh iterations was established as the strict convergence criterion.

As demonstrated in Table 3 and visually confirmed by the asymptotic curve in Figure 5 the peak stress converges rapidly. The transition from Mesh 3 to Mesh 4 yielded a stress variation of only 1.79%, successfully satisfying the sub−5% convergence criterion. Consequently, Mesh 4 (Fineness Level 5) was selected as it provides the optimal balance between computational efficiency and result accuracy. To ensure total consistency, the subsequent optimized geometry was discretized using the exact same validated meshing parameters. The final properties of the 3D model and of the mesh are available in Table 4. Also, the generated mesh can be seen in Figure 6.

The kinematic constraints were defined to replicate the physical mounting of the double wishbone architecture, so rigid fixed supports were applied to the internal cylindrical faces of the two articulation bores, upper arm and lower arm. The boundary condition for these internal cylindrical faces was defined as a "Fixed Support" with a "Deformable" behavior setting in SimScale. The location of the "Fixed Support" is show in Figure 7. In standard FEA, a strictly rigid fixed support locks every individual node, preventing any relative displacement and frequently causing artificial local stiffening (stress singularities).

The "Deformable" formulation, however, relies on multipoint constraints to lock only the average macroscopic movement of the entire face, effectively preventing rigid body motion while permitting individual nodes on that surface to displace relative to one another. This allows the internal bore to naturally ovalize under load, providing a much more accurate representation of the structural compliance.

Table 3. Mesh convergence study for the baseline steering knuckle.

Fineness Level	Elements	Nodes	Peak von Mises Stress	Relative Difference
2	18,348	30,150	121 MPa	-
3	26,387	42,209	131.3 MPa	+8.51%
4	35,237	55,453	139.5 MPa	+6.25%
5	42,642	66,737	142 MPa	+1.79%

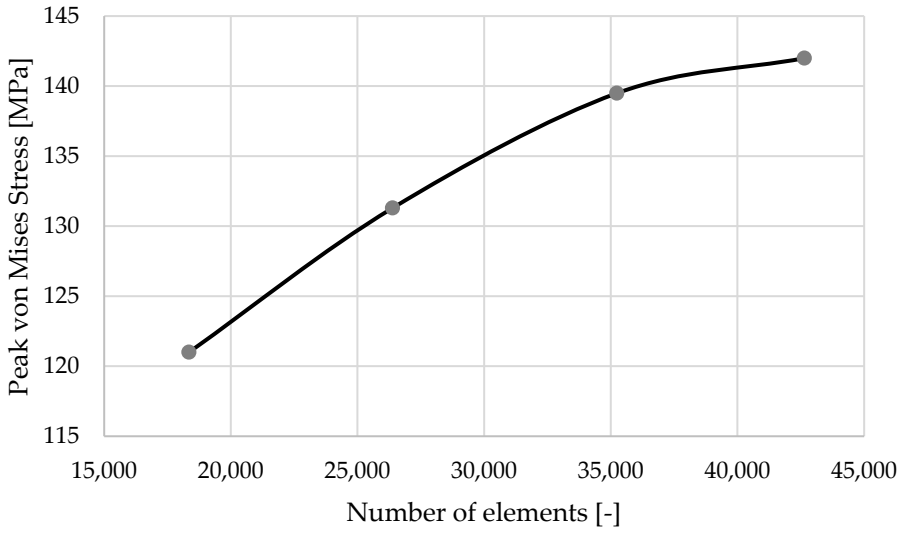


Figure 5. Mesh convergence curve for the baseline model.

Table 4. Three-dimensional model and final mesh properties.

Mesh	
Elements	42,642
Nodes	66,737
3D model	
Properties	Values
Volume	369,996 mm^3
Mass	2.627 kg
X-coordinate center of mass	4.678 mm
Y-coordinate center of mass	13.41 mm
Z-coordinate center of mass	32.52 mm

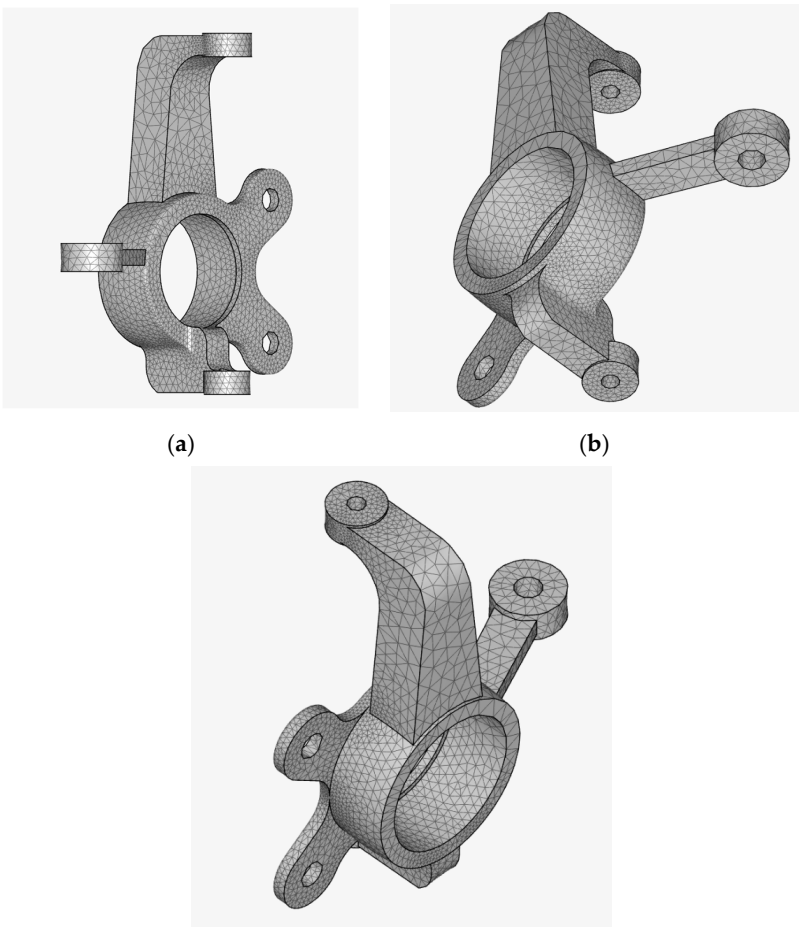


Figure 6. Multiple views of the final mesh of the unoptimized steering knuckle. Three different views of the mesh are shown above (**a**–**c**).

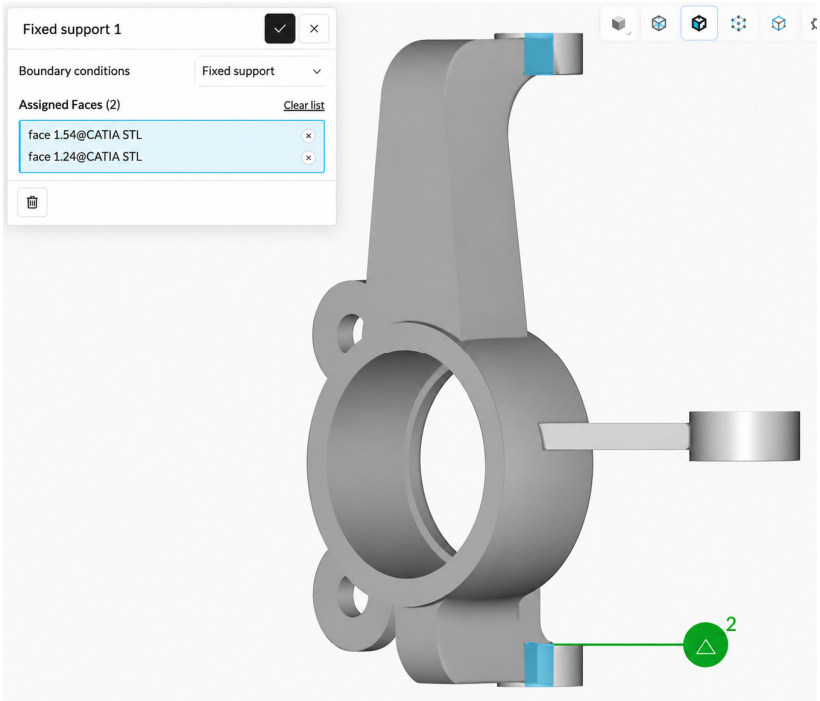


Figure 7. Fixed support's location.

The primary load case introduced in the simulation, shown in Figure 8, corresponds to the dynamic obstacle impact regime, which resulted as the most severe operational scenario. We opted to utilize a Remote Force to simulate the vertical reaction and the longitudinal force exactly at the theoretical tire contact patch. The coordinates of the action point resulted from the dynamic radius (r_d = 265 mm) and the transversal offset (t_o = 45 mm), and the solver automatically calculated and transferred the resultant compound bending and torsional moments to the inner bore of the knuckle.

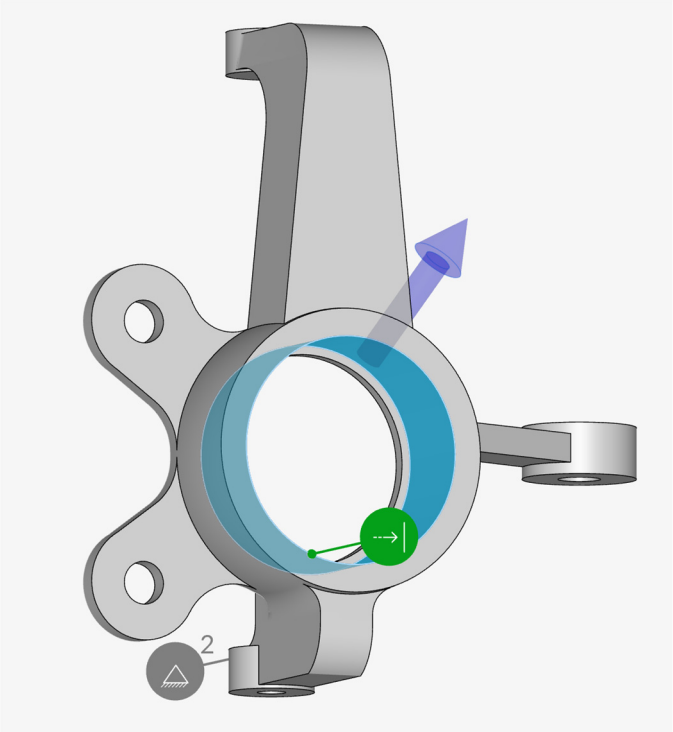


Figure 8. Final load of the steering knuckle.

It is important to distinguish between the material selected for the functional steering knuckle and the material used for the physical geometric prototype. The structural analyses presented in this study were performed using EN-GJS-450-10 nodular cast iron, selected as the reference material for the load-bearing metallic component. The ABS material used in the additive-manufactured prototype was not proposed as a service material for the steering knuckle. It was selected exclusively for rapid geometric and packaging validation because the purpose of the physical prototype was to verify spatial clearances, assembly interfaces, and interference conditions. Therefore, the mechanical performance reported in the FEA results refers to the EN-GJS-450-10 configuration, whereas the ABS prototype is considered only a geometric mock-up.

2.5. Parametric Optimization

We returned to the CATIA modelling environment after the simulation succeeded, where material was strategically subtracted from the non-load-bearing areas through the manual addition of Pocket operations and wall-thinning operations. After, validation runs within SimScale confirmed that this parametric mass reduction significantly decreased the overall volume and unsprung mass of the component while maintaining the stress levels within the accepted safety margins. This optimized, highly efficient geometry is the final digital model of the steering knuckle, fully ready for the Additive Manufacturing packaging validation phase consolidated in the Rapid Prototyping chapter. In the present

study, the term parametric optimization refers to an iterative, FEA-guided manual geometry refinement rather than to an automated mathematical optimization algorithm.

The parametric optimization procedure followed in this study is summarized in Figure 9. The workflow integrates the definition of suspension architecture and loading conditions, parametric CAD modelling, finite element analysis, identification of low-stress regions, iterative geometric modification, and structural re-evaluation until the imposed design constraints are satisfied.

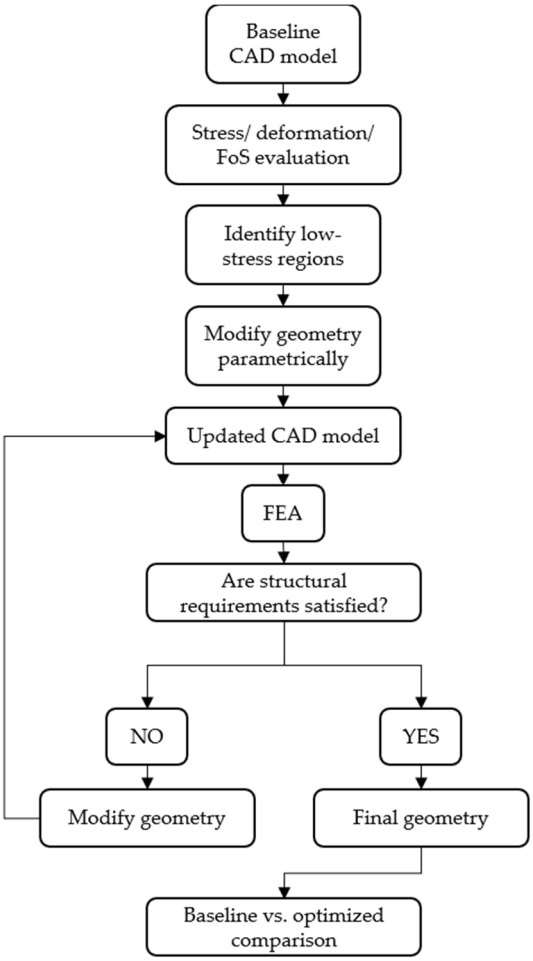


Figure 9. Flowchart of the proposed CAD–FEA-based parametric optimization methodology for the steering knuckle.

While algorithmic topology optimization is highly effective at identifying the absolute theoretical minimum mass, it frequently generates organic, bionic meshes (e.g., STL formats). These complex, irregular geometries typically require extensive reverse-engineering to reconstruct the precise NURBS surfaces necessary for CAM software and CNC machining. To justify the selection of the manual parametric optimization for this specific LCV component, Table 5 summarizes a comparative analysis of the two strategies. The parametric approach was preferred as it preserves the CAD feature tree, allowing enforcement of the 5 mm manufacturing constraints while maintaining an exportable model for production.

The manual iterative material removal was not arbitrary but governed by a strict set of mechanical and manufacturability rules. The threshold for defining a "low-stress region" was established at 30 MPa, which represents approximately 10% of the material's 310 MPa yield strength. In structural optimization theory, specifically within the Solid Isotropic Material with Penalization method, elements exhibiting such low strain energy densities are considered structurally inefficient and are penalized or removed without

compromising global stiffness [54,55]. To ensure the resulting geometry remained viable for conventional manufacturing processes (such as casting or CNC machining), two strict geometric constraints were enforced during material subtraction: a minimum wall thickness of 5 mm was maintained throughout the knuckle to guarantee structural stability, and all newly created internal pockets were blended using a minimum fillet radius of 5 mm (R5) to prevent the introduction of new sharp stress concentrators.

Table 5. Comparative analysis of structural optimization strategies for the steering knuckle.

Feature	Algorithmic Topology Optimization	Manual Parametric Optimization
Mass Reduction	Identifies the absolute theoretical minimum mass distribution.	Achieves significant yet mathematically sub-optimal mass reduction.
Generated Geometry	Organic, irregular mesh surfaces (e.g., STL).	Standard solid body with precise geometric boundaries (NURBS).
CAD Feature Tree	Requires complex reverse-engineering to rebuild functional interfaces.	Fully preserved, allows immediate parametric dimension adjustments.
Manufacturing Rules	Difficult to natively enforce exact standard radius or uniform wall thickness.	Strictly enforces exact manufacturing limits.
Direct Usability	Typically requires surface reconstruction before CAM/CNC programming.	Directly exportable to CAM software for immediate toolpath generation.

To quantify the geometric outcomes of the iterative parametric optimization, a direct comparison between the initial baseline model and the optimized steering knuckle was conducted. The optimized version of the knuckle is shown in Figure 10. By strategically introducing pockets and reducing wall thicknesses in the identified low-stress zones, the overall volume was successfully decreased. The comparative physical properties are detailed in Table 6. As observed, parametric optimization achieved a 10% reduction in unsprung mass, lowering the component's weight from 2.627 kg to 2.364 kg.

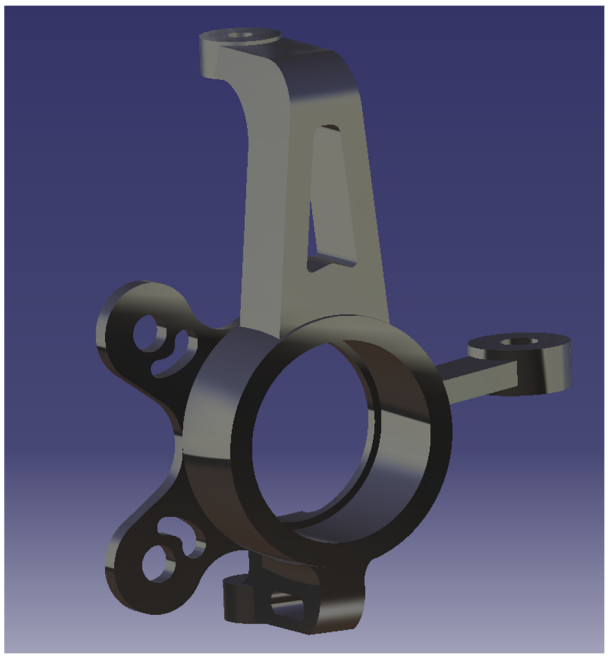


Figure 10. Optimized 3D model of the steering knuckle.

Table 6. Quantitative comparison of volume and mass (baseline vs. optimized).

Parameter	Baseline Model	Optimized Model	Absolute Difference [-]
Volume	369,996 mm^3	332,886 mm^3	-37,110 mm^3
Mass	2.627 kg	2.364 kg	-0.267

2.6. Rapid Prototyping

The optimized digital model of the steering knuckle was exported as a high-resolution 3MF file to preserve maximum topological fidelity. We used Bambu Lab's slicer, Bambu Studio Version 2.7.0.55, to generate the manufacturing instructions, known as G-code, for the printer to make the physical prototype. The primary objective of this phase was not to manufacture a ready-to-use, load-bearing metal component, but rather to fabricate a highly accurate functional mock-up using a technical polymer in the fastest way possible. This physical iteration is generally essential for executing rigorous packaging validation, enabling engineers to physically verify spatial clearances, structural interferences with the brake caliper and wheel rim, and the precise alignment of the suspension hardpoints prior to committing to costly traditional casting methodologies, which would also take a lot of time.

The parameters configured within Bambu Studio were explicitly optimized to balance dimensional accuracy, structural rigidity, and fabrication efficiency and can be seen in Table 7. We chose the Gyroid structure because it is highly advantageous for automotive prototyping as it provides very good isotropic strength. This ensures the component remains rigid during physical handling and suspension assembly testing, despite not being as resistant as a casted component. The Gyroid structure is shown in Figure 11.

Table 7. Three-dimensional printing parameters used for the slicing of the optimized model of the steering knuckle.

3D printer	Bambu Lab P2S
Slicing software	Bambu Studio V2.7.0.55
Material	ABS
Nozzle width	0.4 mm
Infill pattern	Gyroid
Sparse infill density	20%
Support type	Automatic Tree
Threshold angle	30°

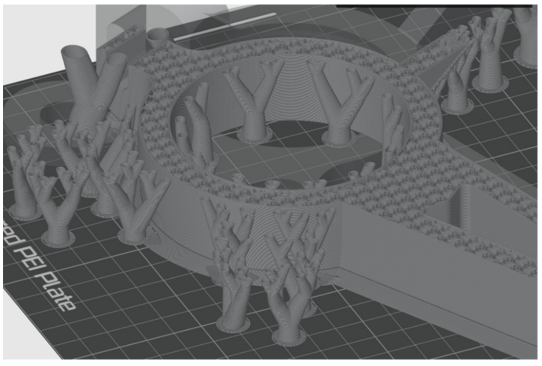


Figure 11. Sliced component mid-section highlights the internal 20% Gyroid infill pattern.

The unavoidable overhangs of the steering knuckle's geometry, under the braking bracket and under the tie-rod mounts, required support, but the slicing software has an automatic function that places support where needed in a matter of seconds. We opted for the automatic tree supports, shown in Figure 12, instead of standard linear structures because this topological approach branches out to support overhanging nodes with minimal contact area on the primary geometry, so it preserves a superior surface finish and facilitates effortless post-processing.

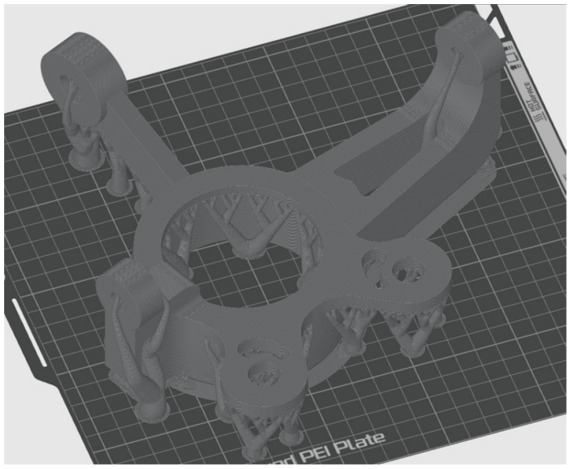


Figure 12. Top view of the sliced geometry with generated tree supports.

We also applied a 10 mm outer brim, shown in Figure 13, to the base layer to guarantee print stability. This bed adhesion technique eliminates the risk of thermal warping and secures the large component to the build plate during the prolonged printing process.

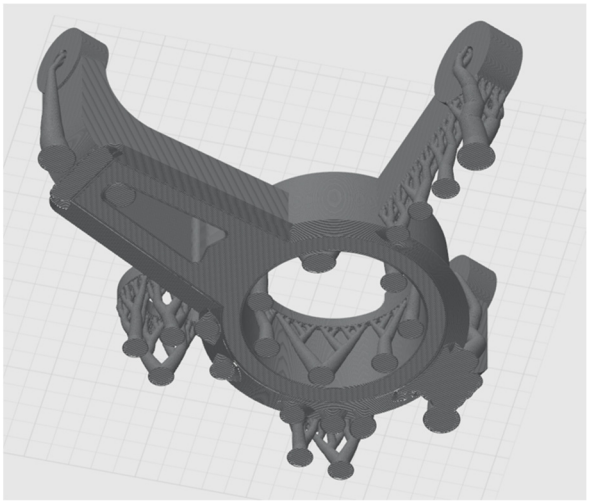


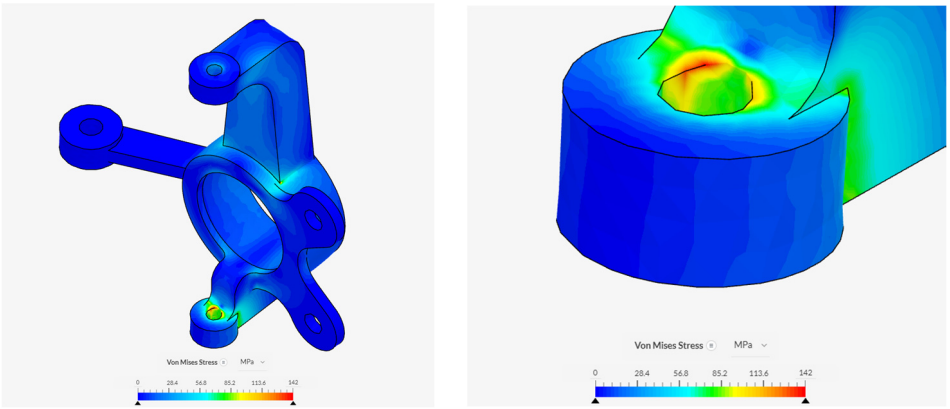
Figure 13. Bottom view illustrates the 10 mm outer brim and footprint.

3. Results

3.1. Structural Validation

The results of the static linear analysis taken from SimScale confirm the structural integrity of the baseline steering knuckle under the most severe dynamic load case. It was expected as the structure was very bulky from the beginning. The SimScale solver computed a maximum equivalent von Mises stress of 142 MPa, which can be seen on the tension map in Figure 14. The maximum stress concentration is localized at the fillet

transition zone connecting the main upright body to the lower control arm mounting bracket as anticipated in high-load structural joints.

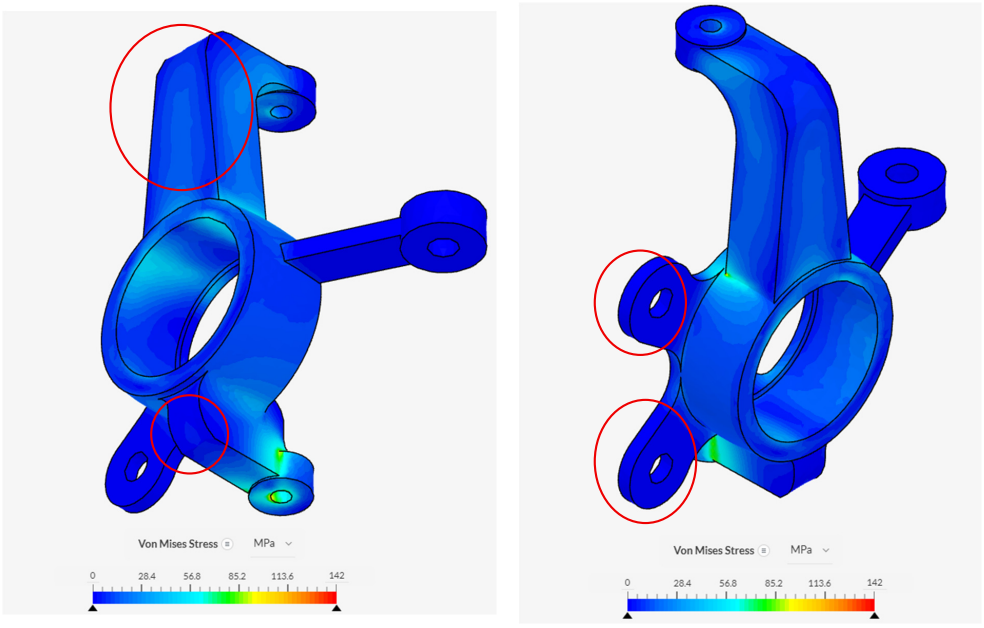


(**a**) (**b**)

Figure 14. Global von Mises stress map: (**a**) overview; (**b**) highlighting the peak tension.

Keeping in mind the selected material, EN-GJS-450-10 nodular cast iron, has a minimum yield strength of 310 MPa, the maximum induced stress of 142 MPa remains safely within the elastic domain, and this state of stress translates to a minimum Factor of Safety of approximately 2.18, demonstrating a robust preliminary design capable of withstanding severe obstacle impact regimes without permanent plastic deformation, which would make the steering knuckle unrepairable.

Following the validation of the baseline structural integrity, the resulting von Mises tension color map was used as a precise diagnostic tool to identify areas where the material experiences negligible stress levels, typically below 30 MPa. Based on this visual data, the iterative parametric optimization was executed. The negligible stress zones can be seen in Figure 15.



(**a**) (**b**)

Figure 15. Global von Mises Stress map highlighting the low-stress zones: (**a**) front left side; (**b**) front right side.

Next, parametric optimization was done, and a new simulation was conducted using the updated geometry of the steering knuckle. The same boundary conditions were used but the 3D model was changed. The results can be observed in the Figure 16.

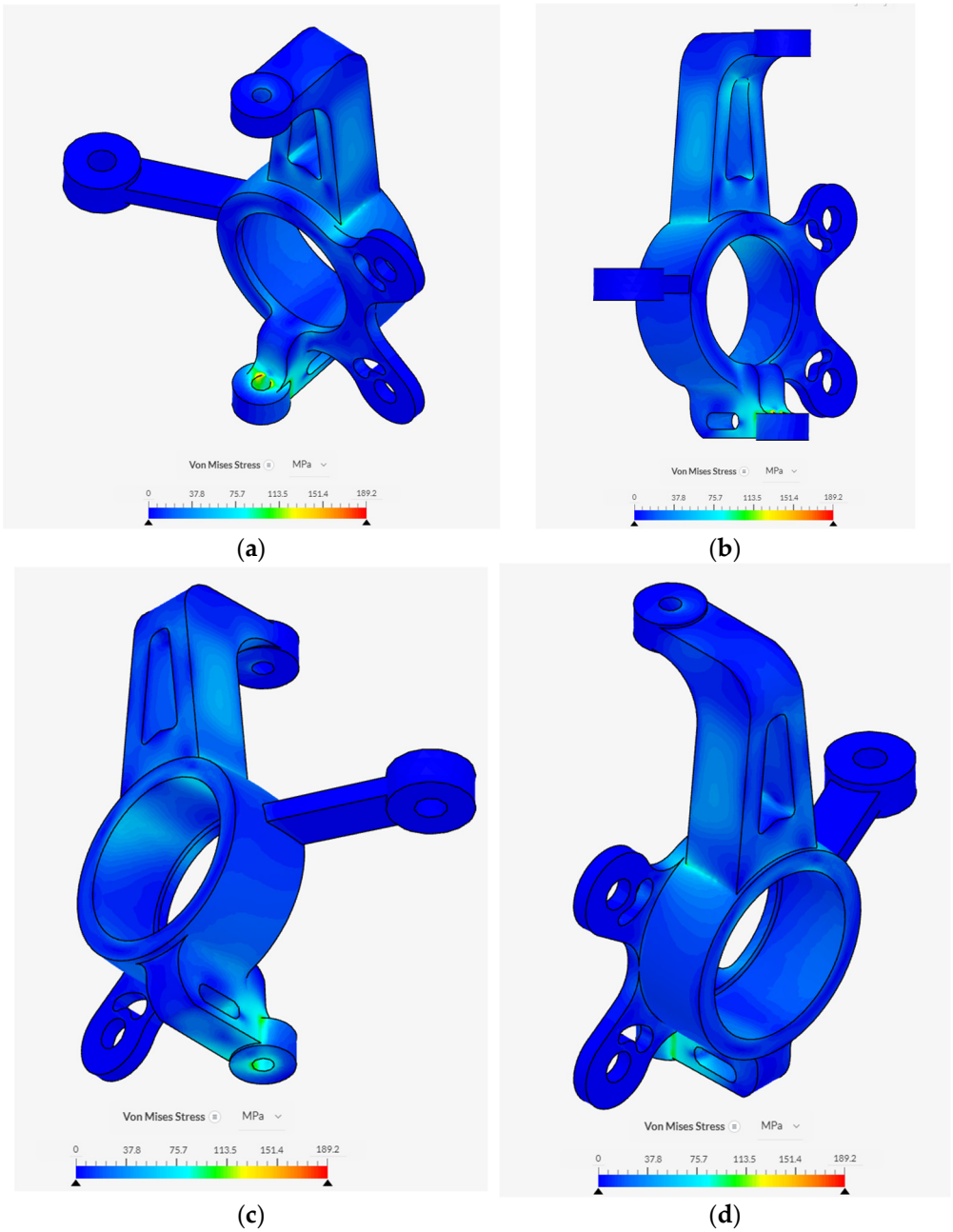


Figure 16. Global von Mises stress map of the optimized steering knuckle: (**a**) back side; (**b**) left back side; (**c**) front left side; (**d**) front right side.

Following the simulation of the optimized geometry, it is imperative to evaluate the structural integrity by calculating the Factor of Safety (FoS). The FoS is determined using the ratio between the material's yield strength (σ_{yield}) and the maximum equivalent von Mises stress (σ_{max}) registered in the component: $FoS = \frac{\sigma_{yield}}{\sigma_{max}}$ [-].

For the selected EN-GJS-450-10 nodular cast iron, the minimum yield strength is σ_{yield} = 310 MPa. Table 8 presents the comparative structural performance between the two design iterations.

Table 8. Quantitative comparison of structural performance (baseline vs. optimized).

Parameter	Baseline Model	Optimized Model	Absolute Difference [-]
Peak von Mises Stress	142 MPa	189.2 MPa	+47.2 MPa
Material Yield Strength	310 MPa	310 MPa	0 MPa
Factor of Safety	2.18	1.64	-0.54

Although the removal of 10% of the material logically caused a localized increase in the peak von Mises stress (from 142 MPa to 189.2 MPa), the maximum stress remains comfortably within the elastic domain of the chosen cast iron. The resulting minimum Factor of Safety of 1.64 proves that the manually optimized steering knuckle is robust enough to withstand the most severe dynamic obstacle impact without undergoing permanent plastic deformation, validating the mass reduction procedure.

3.2. Lead-Time Analysis

To understand the real value of our proposed workflow, we must look directly at the lead times. We broke down exactly how long it takes to go from a finalized digital design to a physical part you can hold and test on the vehicle for any objective the manufacturer has with the component.

By following our Additive Manufacturing route, the time savings become immediately obvious. Once we finished the iterative mass reduction in CAD, exporting the geometry and setting up the slicing parameters took us less than 15 min. After approximately 20 min for printer bed heat-up and stabilization, the high-speed FDM system needed exactly 6.5 h to extrude the functional mock-up, utilizing just 187 g of ABS. After the printer finished, we allowed the part to cool on the build plate for 2.5 h to prevent thermal warping and then spent about twenty minutes manually removing the automatic tree supports and peeling away the 10 mm bed adhesion brim. When all of these are added up: slicing, preparation, printing, cooling, post-processing and a final hour for geometric inspection, the entire physical realization phase took roughly 11 h. We basically condensed the entire prototyping phase into a single working shift.

To physically validate the calculated manufacturing time and to prove the component's readiness for spatial packaging verification, the optimized knuckle was successfully 3D printed (Figure 17). It is crucial to emphasize that this physical experiment was designed exclusively to assess manufacturability, evaluate the 11 h lead time, and provide a geometric mock-up for assembly clearances. The physical strength of the component is not meant to be tested on this polymer mock-up, as ABS cannot replicate the mechanical properties of EN-GJS-450-10 cast iron. FEA validates the EN-GJS-450-10 metallic configuration, and ABS validates geometric/packaging aspects.

In contrast, conventional casting involves a considerably longer sequence of preparation and manufacturing operations. Sand casting requires pattern preparation, mold production, melting and pouring, solidification, shakeout, cleaning, and subsequent finishing operations. In a handbook on casting, John Campbell detailed that producing a functional metal prototype via sand casting involves creating patterns, preparing sand molds, pouring molten metal, and controlled cooling, a metallurgical cycle that typically requires several days to yield a rough component [56]. For a geometrically complex steering knuckle, these operations are further complemented by machining functional surfaces and interfaces, increasing the total prototype lead time [57].



(**a**) (**b**)

Figure 17. Physical realization of the optimized steering knuckle mock-up via ABS 3D printing. (**a**) displays the as-printed steering knuckle mock-up with its necessary tree supports structures intact, while (**b**) presents the final physical prototype after support removal.

An alternative conventional method involves machining the knuckle directly from a solid metal billet, bypassing the casting. This subtractive approach requires specialized multi-axis CNC equipment [58]. Prior to initiating any machine, engineers must dedicate considerable time to programming the complex toolpaths necessary for the component's topology. Designing and fabricating custom fixtures to secure such an irregularly shaped part introduces further production delays [52]. Even with access to a dedicated machine shop, the complete setup and machining cycle for a custom steering knuckle typically results in prototype lead times measured in weeks [52].

Based on the manufacturing sequences described in the referenced literature and the process requirements of the investigated steering knuckle, a comparative assessment of the three investigated routes was established. The proposed FDM additive-manufacturing route required approximately 11 h to obtain the ABS geometric prototype, whereas the conventional casting and CNC-machining routes were estimated at approximately 84 h and 168 h, respectively. These values are not intended to represent manufacturing times for functionally equivalent load-bearing components. Instead, they provide a comparative indication of the time required to obtain a physical representation of the investigated geometry through each manufacturing route. The three approaches serve different purposes within the development process: the FDM prototype enables rapid geometric, packaging, clearance, and assembly verification, while casting and CNC machining can provide metallic prototypes suitable for subsequent structural validation. Therefore, the shorter FDM lead time represents an advantage specifically for early-stage geometric prototyping and design iteration rather than a replacement for conventional metallic manufacturing when a load-bearing component is required. The comparison is summarized in Table 9.

The structural comparison must be interpreted according to the intended purpose of each prototype. The ABS component manufactured by FDM was not intended to reproduce the load-bearing performance of the metallic steering knuckle and was therefore not subjected to structural FEA or mechanical testing. Its value within the proposed workflow lies in the rapid physical verification of geometry, packaging, clearances, and assembly interfaces. In contrast, the casting and CNC-machining routes can produce metallic prototypes using EN-GJS-450-10 nodular cast iron, for which the optimized geometry achieved a maximum von Mises stress of 189.2 MPa and a Factor of Safety of 1.64 in the present FEA configuration. These values should be regarded as numerical predictions for the metallic component and not as experimental measurements of manufactured prototypes. Consequently, the comparison in Table 9 does not establish that one manufacturing route is universally superior to the others. Rather, it highlights the different

roles of rapid polymer prototyping and conventional metallic manufacturing within the component-development process.

Table 9. Comparison of the investigated prototyping and manufacturing routes in terms of lead time and structural applicability.

Criteria	FDM Additive Manufacturing	Sand Casting	CNC Machining
Prototype/component material	ABS polymer	EN-GJS-450-10 nodular cast iron	EN-GJS-450-10 nodular cast iron
Main purpose	Geometric, packaging, clearance, and assembly verification	Functional metallic prototype/component	Functional metallic prototype/component
Manufacturing principle	Layer-by-layer additive deposition	Molding and solidification of molten metal	Subtractive material removal from a solid/semi-finished workpiece
Tooling and process preparation	No dedicated mold required; slicing and printer setup	Pattern/mold preparation and casting setup required	CAM programming, work holding/fixturing, and cutting-tool setup required
Lead time *	11 h	84 h	168 h
Structural applicability of physical prototype	Not intended for load-bearing operation	Capable of producing a load-bearing metallic component, subject to manufacturing quality and experimental validation	Capable of producing a load-bearing metallic component, subject to manufacturing quality and experimental validation
Structural assessment in the present study	Not performed on the ABS prototype	FEA of the EN-GJS-450-10 configuration	FEA of the EN-GJS-450-10 configuration
Maximum von Mises stress **	-	189.2 MPa	189.2 MPa
Factor of Safety **	-	1.64	1.64

* The lead times for casting and CNC machining are comparative estimates and depend on tooling, equipment, material, machining strategy, and production conditions. ** The stress and Factor of Safety values correspond to the optimized geometry modeled using EN-GJS-450-10 nodular cast iron and therefore refer to the functional metallic configuration rather than to the ABS prototype. The 11 h FDM route was investigated as a geometric and packaging prototyping solution; its physical strength was not experimentally or numerically assessed because the printed part contains a non-solid 20% Gyroid infill and was not intended for load-bearing operation.

4. Conclusions

This study successfully demonstrated the implementation of a modern, highly efficient engineering workflow for the development of an automotive steering knuckle, reducing the time gap between analytical kinematic design, virtual structural validation, and rapid physical prototyping.

The finite element analysis confirmed the structural viability of the baseline geometry under the most severe dynamic obstacle impact load. With a peak von Mises stress of 142 MPa, the component maintained a robust Factor of Safety of 2.18 relative to the yield strength of the selected EN-GJS-450-10 nodular cast iron. This structural baseline facilitated data-driven parametric optimization and allows for targeted mass reduction in low-stress regions without compromising the kinematic integrity of the double wishbone architecture.

When compared to recent algorithmic topology optimization studies in the literature (e.g., [6,7]), which often report aggressive mass reductions between 15% and 25%, our achieved mass reduction of 10% is intentionally more conservative. However, unlike bionic designs that necessitate complex five-axis CNC machining or bespoke casting molds, our parametrically optimized geometry completely preserves standard manufacturing rules (R5

fillets, 5 mm minimum wall thickness). This ensures that the component maintains a highly robust Safety Factor of 1.64 while remaining immediately compatible with conventional mass-production techniques.

The transition from the digital environment to Additive Manufacturing highlighted a big shift in prototyping efficiency. By fabricating the functional mock-up in approximately 11 h using minimal polymer material, the project showcased a drastic reduction in development lead times. This rapid turnaround is crucial in the automotive sector, allowing engineers to physically validate spatial packaging, assess component clearances, and verify assembly ergonomics at a fraction of the temporal and financial costs associated with traditional casting or CNC machining. However, it must be explicitly acknowledged that the ABS mock-up was utilized exclusively for spatial and packaging verification. It was not subjected to mechanical or destructive testing, meaning that complete physical validation of the FEA structural predictions still requires a metallic prototype. Figure 18 shows the process proposed in the article from Computer-Aided-Design to Finite Element Analysis and Additive Manufacturing.

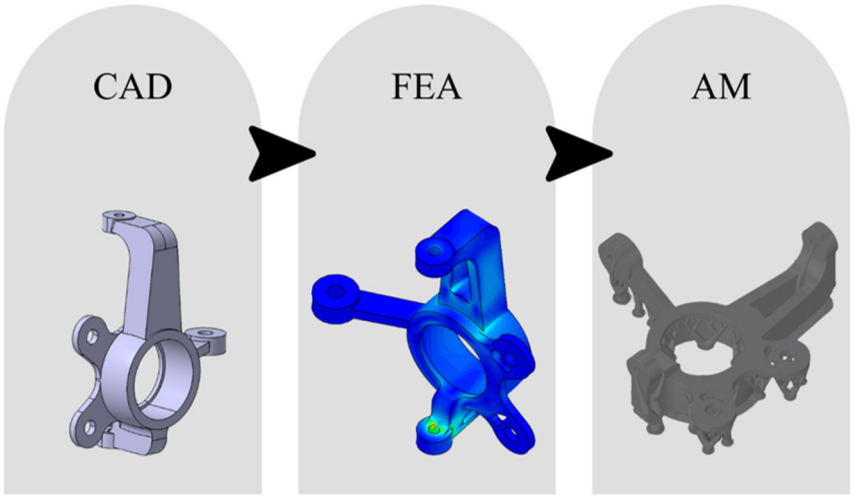


Figure 18. Illustration of the process proposed in the article.

While the proposed workflow successfully demonstrates a significant reduction in geometric prototyping lead time, several limitations of the present study should be acknowledged. The physical prototype was fabricated from ABS polymer using Fused Deposition Modeling and was intended exclusively for geometric, packaging, clearance, and assembly verification. It therefore cannot be considered a functional replacement for a load-bearing metallic steering knuckle and cannot reproduce the mechanical, fatigue, impact, and durability characteristics of the final component. The structural assessment presented in this study was performed numerically using EN-GJS-450-10 nodular cast iron as the reference material for the functional metallic steering knuckle. Consequently, the structural performance of the optimized geometry has not yet been experimentally validated using a metallic prototype under static, fatigue, or representative vehicle operating conditions. The reported FEA results should therefore be interpreted as numerical structural validation rather than complete experimental validation of the final component. To address these limitations, future work will focus on the experimental validation of the optimized steering-knuckle geometry using a metallic prototype manufactured from a material suitable for the intended service conditions. In particular, the EN-GJS-450-10 nodular cast iron configuration investigated in the present study will be considered for experimental correlation of the numerical results through static and fatigue testing, followed by validation under representative vehicle operating conditions. Such experimental

testing will provide the necessary correlation between the FEA predictions and the actual structural and durability response of the component. In addition, future investigations may consider alternative manufacturing technologies and advanced optimization methods to further improve the stiffness-to-weight ratio while maintaining the required structural and manufacturing constraints.

Author Contributions: Conceptualization, V.-C.M. and A.D.; methodology, V.-C.M. and A.D.; software, V.-C.M., A.D. and G.B.; validation, A.D., V.-C.M., G.B. and R.-A.D.; formal analysis, R.-A.D. and A.D.; investigation, V.-C.M., A.D. and R.-A.D.; resources, V.-C.M., A.D.; data curation, V.-C.M., A.D., G.B. and R.-A.D.; writing—original draft preparation, V.-C.M. and A.D.; writing—review and editing, A.D., V.-C.M., G.B. and R.-A.D.; visualization, V.-C.M. and A.D.; supervision, A.D.; project administration, A.D.; funding acquisition, A.D. and R.-A.D. All authors have read and agreed to the published version of the manuscript.

Funding: The APC was funded by the National University of Science and Technology POLITEHNICA Bucharest from its own funds.

Data Availability Statement: The data presented in this study are available upon request from the corresponding author.

Acknowledgments: This work was supported by a grant from the National Program for Research of the National Association of Technical Universities—GNAC ARUT 2023.

Conflicts of Interest: The authors declare no conflicts of interest.

Abbreviations

The following abbreviations are used in this manuscript:

LCV	Light Commercial Vehicle
CAD	Computer-Aided Design
FEA	Finite Element Analysis
AM	Additive Manufacturing
FDM	Fused Deposition Modeling
PBF	Powder Bed Fusion
CNC	Computer Numerical Control
NURBS	Non-Uniform Rational B-Spline
CAM	Computer-Aided Manufacturing software

References

1. Milliken, W.F.; Milliken, D.L. *Race Car Vehicle Dynamics*; SAE International: Warrendale, PA, USA, 1995.
2. Happian-Smith, J. *An Introduction to Modern Vehicle Design*; Butterworth-Heinemann: Oxford, UK, 2001.
3. Jazar, R.N. *Vehicle Dynamics: Theory and Application*, 3rd ed.; Springer: Cham, Switzerland, 2017. [CrossRef]
4. Arshad, M.W.; Lodi, S.; Liu, D.Q. Double Wishbone Suspension: A Computational Framework for Parametric 3D Kinematic Modeling and Simulation Using Mathematica. *Technologies* **2025**, *13*, 332. [CrossRef]
5. Tanik, E.; Parlaktaş, V. On the analysis of double wishbone suspension regarding steering input and anti-dive/lift effect. *J. Adv. Mech. Des. Syst. Manuf.* **2016**, *10*, JAMDSM0032. [CrossRef]
6. Hasan, A.; Lu, C.; Liu, W. Lightweight Design and Analysis of Steering Knuckle of Formula Student Car Using Topology Optimization Method. *World Electr. Veh. J.* **2023**, *14*, 233. [CrossRef]
7. Almonti, D.; Salvi, D.; Mingione, E.; Vesco, S. Lightweight and Sustainable Steering Knuckle via Topology Optimization and Rapid Investment Casting. *J. Manuf. Mater. Process.* **2025**, *9*, 252. [CrossRef]
8. Dusane, S.V.; Dipke, M.K.; Kumbhalkar, M.A. Analysis of Steering Knuckle of All Terrain Vehicles (ATV) Using Finite Element Analysis. *IOP Conf. Ser. Mater. Sci. Eng.* **2016**, *149*, 012133. [CrossRef]
9. Thompson, M.K.; Moroni, G.; Vanacker, T.; Fadel, G.; Campbell, R.I.; Gibson, I.; Bernard, A.; Schulz, J.; Graf, P.; Ahuja, B.; et al. Design for Additive Manufacturing: Trends, Opportunities, Considerations, and Constraints. *CIRP Ann. Manuf. Technol.* **2016**, *65*, 737–760. [CrossRef]

10. Vido, M.; Cardoso de Oliveira Neto, G.; Lourenço, S.R.; Amorim, M.; Rodrigues, M.J.F. Computer-Aided Design and Additive Manufacturing for Automotive Prototypes: A Review. *Appl. Sci.* **2024**, *14*, 7155. [CrossRef]
11. Sancibrian, R.; García, P.; Viadero, F.; Fernández, A.; De-Juan, A. Kinematic Design of Double-Wishbone Suspension Systems Using a Multiobjective Optimisation Approach. *Veh. Syst. Dyn.* **2010**, *48*, 793–813. [CrossRef]
12. Reddy, K.V.; Kodati, M.; Chatra, K.; Bandyopadhyay, S. A Comprehensive Kinematic Analysis of the Double Wishbone and MacPherson Strut Suspension Systems. *Mech. Mach. Theory* **2016**, *105*, 441–470. [CrossRef]
13. Chen, J.; Zhao, Z.; Su, Y.; Huang, J.; Gan, Y. Analysis and Optimization of Wheel Alignment Parameters for Double Wishbone Suspension of Distributed Electric-Driven Lunar Rover. *Appl. Sci.* **2026**, *16*, 2798. [CrossRef]
14. Zhang, S.; Gao, Y.; Gao, D.; Pan, T. *The Multi-Objective Optimization Design of Hard Point Parameters for Double Wishbone Independent Suspension*; SAE International: Detroit, MI, USA, 2023. [CrossRef]
15. Sun, S.; Zhu, Y.; Du, J.; Jiang, Z. Kinematic Performance Optimization of Double Wishbone Suspension Based on ADAMS. In *Intelligent Equipment and Special Robots*; IOS Press: Amsterdam, The Netherlands, 2024; pp. 174–179. [CrossRef]
16. Țoțu, V.; Alexandru, C. Multi-Criteria Kinematic Optimization of a Double Wishbone Suspension Mechanism. *Acta Tech. Napoc. Ser. Appl. Math. Mech. Eng.* **2025**, *69*, 249–258.
17. Niu, Z.; Liu, S.; Li, B.; Pan, Z.; Wang, R. Explicit Solution to the Nonlinear Geometry of Double Wishbone Suspension by Decoupling Steering and Wheel Jumping DOF. *Proc. Inst. Mech. Eng. Part D J. Automob. Eng.* **2025**, *239*, 1327–1340. [CrossRef]
18. Archut, J.-L.; Corves, B. Real-Time Multibody Simulation of Vehicle Wheel Suspensions of Different Topologies with Elastokinematic Properties. *Multibody Syst. Dyn.* **2025**, *63*, 255–271. [CrossRef]
19. Llopis-Albert, C.; Rubio Montoya, F.J.; Zeng, S. Multiobjective Optimization Framework for Designing a Vehicle Suspension System. A Comparison of Optimization Algorithms. *Adv. Eng. Softw.* **2023**, *176*, 103375. [CrossRef]
20. Nishikawa, K.; Shintani, K.; Iwata, M.; Miyaki, K. Suggest of Set-Based Design Method Based Differential Evolution and Application to Design of Suspension. *Trans. Soc. Automot. Eng. Jpn.* **2023**, *54*, 1121–1126. [CrossRef]
21. Kim, K.J. Light-Weight Design and Fatigue Characteristics of Automotive Knuckle by Using Finite Element Analysis. *J. Mech. Sci. Technol.* **2021**, *35*, 2989–2995. [CrossRef]
22. Kashyzadeh, K.R.; Souri, K.; Gharehsheikh Bayat, A.; Safavi Jabalbarez, R.; Ahmad, M. Fatigue Life Analysis of Automotive Cast Iron Knuckle under Constant and Variable Amplitude Loading Conditions. *Appl. Mech.* **2022**, *3*, 517–532. [CrossRef]
23. Kashyzadeh, K.R.; Farrahi, G.H. Improvement of HCF Life of Automotive Safety Components Considering a Novel Design of Wheel Alignment Based on a Hybrid Multibody Dynamic, Finite Element, and Data Mining Techniques. *Eng. Fail. Anal.* **2023**, *143*, 106932. [CrossRef]
24. Akilan, S.; Reddy, K.J. Design Improvement of Steering Knuckle through Topology Optimization for Additive Manufacturing. *Cogent Eng.* **2024**, *11*, 2416487. [CrossRef]
25. Borda, F.; La Rosa, A.D.; Filice, L.; Gagliardi, F. Environmental Impact of Process Constrained Topology Optimization Design on Automotive Component' Life. *Int. J. Mater. Form.* **2023**, *16*, 48. [CrossRef]
26. Du, X.; Liang, H. Lightweight Design of Automotive Front Rail Based on Topology Optimisation and Collision Analysis. *Int. J. Crashworthiness* **2024**, *29*, 402–413. [CrossRef]
27. Santana, C.; Reyes-Osorio, L.; Orona-Hinojos, J.; Huerta, L.; Rios, A.; Zambrano-Robledo, P. Numerical Study of Reinforced Aluminum Composites for Steering Knuckles in Last-Mile Electric Vehicles. *World Electr. Veh. J.* **2024**, *15*, 109. [CrossRef]
28. Li, F.; Sun, J.; Bao, J.; Yang, J.; Li, H.; Zhong, C.; Gao, Y.; He, Q.; Xie, K.; Li, W. Failure Analysis of Truck Steering Knuckle. *Eng. Fail. Anal.* **2022**, *140*, 106537. [CrossRef]
29. Çelik, A.; Yıldız, A.R. Otomobil Salıncak Kolunun Yapısal Analiz ve Optimizasyon Teknikleri ile Ağırlık Azaltılması [Weight Reduction of an Automotive Wishbone Using Structural Analysis and Optimization Techniques]. *Bursa Uludağ Üniv. Mühendis. Fakültesi Derg.* **2022**, *27*, 817–830. [CrossRef]
30. Wu, N.; Liu, C.; Yang, Z.; Lian, Z. Structural Design of Special Vehicle Components Based on Topology Optimization. *Int. J. Automot. Technol.* **2023**, *24*, 541–549. [CrossRef]
31. Yang, J.; Li, B.; Liu, J.; Tu, Z.; Wu, X. Application of Additive Manufacturing in the Automobile Industry: A Mini Review. *Processes* **2024**, *12*, 1101. [CrossRef]
32. Wawryniuk, Z.; Brancewicz-Steinmetz, E.; Sawicki, J. Revolutionizing Transportation: An Overview of 3D Printing in Aviation, Automotive, and Space Industries. *Int. J. Adv. Manuf. Technol.* **2024**, *134*, 3083–3105. [CrossRef]
33. Sarzyński, B.; Śnieżek, L.; Grzelak, K. Metal Additive Manufacturing (MAM) Applications in Production of Vehicle Parts and Components—A Review. *Metals* **2024**, *14*, 195. [CrossRef]
34. Priarone, P.C.; Catalano, A.R.; Settineri, L. Additive Manufacturing for the Automotive Industry: On the Life-Cycle Environmental Implications of Material Substitution and Lightweighting through Re-Design. *Prog. Addit. Manuf.* **2023**, *8*, 1229–1240. [CrossRef]
35. Hamza, A.; Bousnina, K.; Dridi, I.; Ben Yahia, N. Revolutionizing Automotive Design: The Impact of Additive Manufacturing. *Designs* **2025**, *9*, 24. [CrossRef]

36. Fischer, L.A.S.; Foggiatto, J.A.; Marcondes, P.V.P.; Lajarin, S.F. Design for Additive Manufacturing (DFAM) Applied in the Manufacture of Master Sample for the Automotive Industry. *Proc. Inst. Mech. Eng. Part D J. Automob. Eng.* **2025**, *239*, 96–103. [CrossRef]
37. Dash, S.; Nordin, A.; Johansson, G. Dual Design for Additive Manufacturing in Engineering Design: A Systematic Literature Review. *Rapid Prototyp. J.* **2025**, *31*, 40–61. [CrossRef]
38. Lkadi, O.; Abouhazim, S.; Nassraoui, M.; Otmane, B. A Comprehensive Design Framework for Additive Manufacturing in the Automotive Industry: A Case Study. *Arch. Mater. Sci. Eng.* **2024**, *124*, 57–64. [CrossRef]
39. Streparava, S.C.; Ferraresi, R.; Magni, M.; Guerini, L.; Cornacchia, G. Evolution of Prototyping in Automotive Engineering: A Comprehensive Study on the Reliability of Additive Manufacturing for Advanced Powertrain Components. *Frat. Integrità Strutt.* **2024**, *18*, 85–99. [CrossRef]
40. Alami, A.H.; Olabi, A.G.; Alashkar, A.; Alasad, S.; Aljaghoub, H.; Rezk, H.; Abdelkareem, M.A. Additive Manufacturing in the Aerospace and Automotive Industries: Recent Trends and Role in Achieving Sustainable Development Goals. *Ain Shams Eng. J.* **2023**, *14*, 102516. [CrossRef]
41. Trovato, M.; Belluomo, L.; Bici, M.; Prist, M.; Campana, F.; Cicconi, P. Machine Learning in Design for Additive Manufacturing: A State-of-the-Art Discussion for a Support Tool in Product Design Lifecycle. *Int. J. Adv. Manuf. Technol.* **2025**, *137*, 2157–2180. [CrossRef]
42. Favi, C.; Murgese, L.; Villazzi, N.; Gallozzi, S.; Mandolini, M.; Marconi, M. Integrating Life Cycle Engineering into Design for Additive Manufacturing: A Review. *J. Manuf. Syst.* **2025**, *82*, 599–631. [CrossRef]
43. Ben Amor, S.; Elloumi, N.; Eltaief, A.; Louhichi, B.; Alrasheedi, N.H.; Seibi, A. Digital Twin Implementation in Additive Manufacturing: A Comprehensive Review. *Processes* **2024**, *12*, 1062. [CrossRef]
44. Celik, H.K.; Elham, A.; Cinar, R.; Erbil, M.A.; Entwistle, R.; Rennie, A.E.W.; Akinci, I. Development of a CAD–FEA Integrated Automation Add-In for DfAM-Aware Topology Optimization: A Case Study on an Additively Manufactured Pusher Duct Support Bracket for a Novel UAV Prototype. *Appl. Sci.* **2025**, *15*, 12341. [CrossRef]
45. Soori, M.; Karimi Ghaleh Jough, F.; Dastres, R.; Arezoo, B. Additive Manufacturing Modification by Artificial Intelligence, Machine Learning, and Deep Learning: A Review. *Addit. Manuf. Front.* **2025**, *4*, 200198. [CrossRef]
46. Trovato, M.; Vigna, A.; Cicconi, P.; Belluomo, L.; Bici, M.; Campana, F. Analyzing Tools and Methods in Design for Additive Manufacturing: Workflow and Test Cases. *Comput. Aided Des. Appl.* **2025**, *22*, 6. [CrossRef]
47. García-Domínguez, A.; Claver, J.; Camacho, A.M.; Sebastián, M.A. Computational Design Methodology for Additive Manufacturing to Enhance Customised Products and Process Management Efficiency. *Results Eng.* **2025**, *27*, 105480. [CrossRef]
48. Wang, J.; Papadopoulos, P. Finite Element Analysis-Enabled Optimization of Process Parameters in Additive Manufacturing. *Finite Elem. Anal. Des.* **2025**, *244*, 104282. [CrossRef]
49. Daoud, M.A.; Haouari, K.B.; Mechkouri, M.H.; Ennawaoui, A.; El Hadraoui, H.; Naser, I.; Ouardouz, M.; Reklaoui, K. Optimizing Additive Manufacturing Workflows Using Model-Based Systems Engineering. *Results Eng.* **2025**, *27*, 105926. [CrossRef]
50. Zhou, L.; Miller, J.; Vezza, J.; Mayster, M.; Raffay, M.; Justice, Q.; Al Tamimi, Z.; Hansotte, G.; Sunkara, L.D.; Bernat, J. Additive Manufacturing: A Comprehensive Review. *Sensors* **2024**, *24*, 2668. [CrossRef] [PubMed]
51. Borg, L.T. An Approach to Using Finite Element Models to Predict Suspension Member Loads in a Formula SAE Vehicle. Master's Thesis, Virginia Polytechnic Institute and State University, Blacksburg, VA, USA, 2009.
52. Altintas, Y. *Manufacturing Automation: Metal Cutting Mechanics, Machine Tool Vibrations, and CNC Design*, 2nd ed.; Cambridge University Press: Cambridge, UK, 2012. [CrossRef]
53. Cook, R.D.; Malkus, D.S.; Plesha, M.E.; Witt, R.J. *Concepts and Applications of Finite Element Analysis*, 4th ed.; John Wiley & Sons: New York, NY, USA, 2001; pp. 335–342.
54. Bendsøe, M.P.; Sigmund, O. *Topology Optimization: Theory, Methods, and Applications*; Springer: Berlin/Heidelberg, Germany, 2003. [CrossRef]
55. Budynas, R.G.; Nisbett, J.K. *Shigley's Mechanical Engineering Design*, 11th ed.; McGraw-Hill Education: New York, NY, USA, 2019.
56. Campbell, J. *Complete Casting Handbook: Metal Casting Processes, Metallurgy, Techniques and Design*, 2nd ed.; Butterworth-Heinemann: Oxford, UK, 2015. [CrossRef]
57. Kalpakjian, S.; Schmid, S.R. *Manufacturing Engineering and Technology*, 8th ed.; Pearson: Hoboken, NJ, USA, 2020.
58. Groover, M.P. *Fundamentals of Modern Manufacturing: Materials, Processes, and Systems*, 7th ed.; John Wiley & Sons: Hoboken, NJ, USA, 2020.

Disclaimer/Publisher's Note: The statements, opinions and data contained in all publications are solely those of the individual author(s) and contributor(s) and not of MDPI and/or the editor(s). MDPI and/or the editor(s) disclaim responsibility for any injury to people or property resulting from any ideas, methods, instructions or products referred to in the content.